Interval Approaches to Reliable Control of Dynamical Systems

Andreas Rauh[1] and Ekaterina Auer[2]

[1] Chair of Mechatronics, University of Rostock
D-18059 Rostock, Germany
andreas.rauh@uni-rostock.de
[2] Faculty of Engineering, INKO, University of Duisburg-Essen
D-47048 Duisburg, Germany
auer@inf.uni-due.de

Abstract. In recent years, powerful interval arithmetic tools have been developed for the computation of guaranteed enclosures of the sets of all reachable states for dynamical systems. In such simulations, uncertainties in initial conditions and parameters are considered in terms of intervals which contain their complete possible range. The resulting enclosures are verified in the sense that all reachable states are guaranteed to be inside these bounds. For that purpose, both the influence of the above-mentioned uncertainties and numerical inaccuracies arising from computer implementations using finite-precision floating-point arithmetic are taken into account. In this contribution, we present a computational framework for both offline and online applications of interval tools in control design. We summarize verified computational procedures and their application to the solution of initial value problems for both ordinary differential equations and differential algebraic equations. These algorithms are employed for feedforward control design as well as state and disturbance estimation for a distributed heating system. An extension of a basic experimental setup for this system and its corresponding mathematical model are used to describe directions for future research.

1 Introduction

The basis of the methods summarized in this paper are interval techniques which were developed to quantify rounding errors in finite-precision floating-point arithmetic as well as to determine the influence of uncertainties in mathematical system models [8,17]. For technical applications, these models are given either by sets of algebraic equations, discrete-time difference equations, ordinary differential equations (ODEs), differential-algebraic equations (DAEs), or partial differential equations (PDEs).

Software libraries for basic interval arithmetic functionalities such as the evaluation of arithmetic operations and functions (e.g. trigonometric and other transcendental functions) are, for instance, the C++ toolboxes PROFIL/BIAS [9] and FILIB++ [14]. In addition, most verified computational algorithms, such as

Dagstuhl Seminar Proceedings 09471
Computer-assisted proofs - tools, methods and applications
http://drops.dagstuhl.de/opus/volltexte/2010/2512

those presented in this article, make use of partial derivatives of the first and higher orders as well as Taylor coefficients. Such derivatives can be obtained with the help of algorithmic differentiation [7]. The C++ library that is used for this purpose in this contribution is FADBAD++ [2].

On the basis of these software libraries, routines for verified integration of initial value problems (IVPs) for sets of ODEs were developed. Examples for interval-based tools are VNODE-LP [18] and VALENCIA-IVP [1]. In addition, program packages such as VSPODE [15] and COSY VI [3] make use of Taylor model arithmetic in order to reduce the influence of overestimation. Overestimation is a general problem of verified computations. Its meaning is that enclosures of the desired solutions might get too conservative for practical purposes. It often arises if naive implementations of interval algorithms are applied.

On the one hand, packages for verified simulation of dynamical systems build the basis for offline approaches for verification, design, stability analysis and optimization of robust open-loop and closed-loop control strategies (cf. [26, 27, 31–33]). On the other hand, they are also applicable under certain prerequisites to the online computation of feedforward control strategies as well as state and disturbance estimates.

In offline applications, interval tools are used to quantify the effects of uncertainties which result from, for example, manufacturing tolerances or measurement errors occurring unavoidably in any technical application. In the offline design and proof of feasibility, verified enclosures of *all possibly admissible* solutions of control synthesis are determined after verified enclosures of *all reachable* states have been calculated. In this case, the actual computing time is of minor importance. In online applications, however, we have to fulfill given real-time requirements. For that reason, the computation is restricted to determining only one guaranteed admissible solution taking into account the influence of all possible uncertainties in such a way that constraints on state and control variables are not violated. In addition to directly solving IVPs for ODEs or DAEs over sufficiently short time intervals, verified sensitivity analysis (implemented, for example, in VALENCIA-IVP) can be applied to solve this problem. The sensitivity analysis provides a means for the online adjustment of control strategies. For that purpose, the sensitivity of the outputs (as well as the inputs) of a dynamical system with respect to its control inputs (and the desired output) as well as uncertain parameters can be investigated [29, 30].

Verified simulation algorithms for sets of ODEs and DAEs are summarized in the Sections 2 and 3, respectively. In Section 4, DAE-based solution procedures for feedforward control synthesis as well as state and disturbance estimation are presented for finite-dimensional system models. The stability of feedback control structures consisting of independently designed controllers and state estimators is not guaranteed for nonlinear systems. For that reason, suitable procedures for a verified stability analysis and for the computation of guaranteed regions of attraction of stable operating points are necessary as summarized in Section 5. The strategies for feedforward control design and state estimation are applied in real-time to a finite volume representation of a distributed heating system

in Section 6. In Sections 7 and 8 we discuss the task of exact feedback control for a modification of the basic heating system and other control tasks for which dynamic extensions of the state equations are required. These problems include the control of non-quasi-linear sets of DAEs and multiple-input multiple-output systems. Conclusions and an outlook on future work are given in Section 9.

2 Verified Simulation of ODEs in VALENCIA-IVP

In this section, we consider the verified solution of IVPs to the set of ODEs

$$\dot{x}\left(t\right) = f\left(x\left(t\right), t\right) \;\; , \;\; x \in \mathbb{R}^{n_x} \tag{1}$$

with the uncertain initial conditions $x\left(0\right) \in \left[x\left(0\right)\right] := \left[\underline{x}\left(0\right) ; \overline{x}\left(0\right)\right]$, $\underline{x}_i\left(0\right) \leq \overline{x}_i\left(0\right)$ for all $i = 1, \ldots, n_x$ with the help of the verified solver VALENCIA-IVP.

In the basic version of VALENCIA-IVP, time-varying state enclosures

$$\left[x_{encl}\left(t\right)\right] := x_{app}\left(t\right) + \left[R\left(t\right)\right] \tag{2}$$

are computed iteratively which consist of a non-verified approximate solution $x_{app}\left(t\right)$ with guaranteed error bounds $\left[R\left(t\right)\right]$. For the sake of simplicity, we specify the iteration formulas for the ODE (1) in the time interval $0 \leq t \leq T$. In this case, an interval containing the derivatives $\left[\dot{R}(t)\right]$ of the desired error bounds $[R(t)]$ can be computed by

$$\begin{aligned} \left[\dot{R}^{(\kappa+1)}\left(t\right)\right] &= -\dot{x}_{app}\left(t\right) + f\left(\left[x_{encl}^{(\kappa)}\left(t\right)\right], t\right) \\ &= -\dot{x}_{app}\left(t\right) + f\left(x_{app}\left(t\right) + \left[R^{(\kappa)}\left(t\right)\right], t\right) =: r\left(\left[R^{(\kappa)}\left(t\right)\right], t\right) \end{aligned} \tag{3}$$

if

$$\left[\dot{R}^{(\kappa+1)}\left(t\right)\right] \subseteq \left[\dot{R}^{(\kappa)}\left(t\right)\right] \tag{4}$$

holds with

$$\left[R^{(\kappa+1)}\left(t\right)\right] \subseteq \left[R^{(\kappa+1)}\left(0\right)\right] + t \cdot r\left(\left[R^{(\kappa)}\left(\left[0\;;\;t\right]\right)\right], \left[0\;;\;t\right]\right) \tag{5}$$

and $t = T$ as well as $\left[x\left(0\right)\right] \subseteq x_{app}\left(0\right) + \left[R^{(\kappa+1)}\left(t\right)\right]$.

In addition, we can apply the approach of computing exponential state enclosures to prevent the growth of interval diameters for asymptotically stable systems. The basic idea is to use the representation

$$\left[x_{encl}\left(t\right)\right] := \exp\left(\left[\Lambda\right] \cdot t\right) \cdot \left[x_{encl}\left(0\right)\right] \tag{6}$$

for the guaranteed state enclosures with the diagonal matrix

$$\left[\Lambda\right] := \operatorname{diag}\left\{\left[\lambda_i\right]\right\} \;\; , \tag{7}$$

where the coefficients $[\lambda_i]$ are computed iteratively by

$$\left[\lambda_i^{(\kappa+1)}\right] := \frac{f_i\left(\exp\left(\left[A^{(\kappa)}\right]\cdot[0\ ;\ T]\right)\cdot[x_{encl}\,(0)]\,,[0\ ;\ T]\right)}{\exp\left(\left[\lambda_i^{(\kappa)}\right]\cdot[0\ ;\ T]\right)\cdot[x_{encl,i}\,(0)]} \tag{8}$$

for all $i = 1, \ldots, n_x$ in the case of convergence, that means, for $\left[\lambda_i^{(\kappa+1)}\right] \subseteq \left[\lambda_i^{(\kappa)}\right]$.

The iteration formula (8) is only admissible if the value zero does not belong to the set of all reachable states in the time interval $[0\ ;\ T]$. To check this property, we compute guaranteed enclosures for all states by the basic iteration formulas (3)–(5) before evaluating the tighter exponential state enclosures.

A detailed derivation of the iteration formulas of VALENCIA-IVP can be found, for example, in [1,26]. To further tighten the computed state enclosures, consistency tests are available which exclude domains resulting from overestimation by constraint propagation based on conservation properties obtained from suitable balance equations such as energy balances for mechanical systems [6,25]. In control systems, the above-mentioned algorithms can be used to prove whether the enclosures of all reachable states remain within given bounds for known control strategies. In the case of feedback control, it is moreover possible to show whether the resulting control $u\,(x\,(t))$ (given by analytic expressions) matches the corresponding physical constraints on $u\,(t)$.

3 Verified Solution of IVPs for DAEs in VALENCIA-IVP

In this section, we consider semi-explicit DAEs

$$\dot{x}\,(t) = f\,(x\,(t)\,, y\,(t)\,, t) \tag{9}$$

$$0 = g\,(x\,(t)\,, y\,(t)\,, t) \tag{10}$$

with $f : D \mapsto \mathbb{R}^{n_x}$, $g : D \mapsto \mathbb{R}^{n_y}, D \subset \mathbb{R}^{n_x} \times \mathbb{R}^{n_y} \times \mathbb{R}^1$, and the consistent initial conditions $x\,(0)$ and $y\,(0)$. As for the ODEs in Section 2, these DAEs may further depend on uncertain parameters p. To simplify the notation, the dependency on p is not explicitly denoted. However, all presented results are also applicable to $p_i \in \left[\underline{p}_i\ ;\ \overline{p}_i\right]$ with $\underline{p}_i < \overline{p}_i$, $i = 1, \ldots, n_p$. The basis for the applications in Sections 6–8 is the computation of guaranteed enclosures for both consistent initial conditions and solutions to IVPs for DAEs. The enclosures for the differential and algebraic variables $x_i\,(t)$ and $y_j\,(t)$, respectively, are defined by

$$[x_i\,(t)] := x_{app,i}\,(t_k) + (t - t_k)\cdot\dot{x}_{app,i}\,(t_k) + [R_{x,i}\,(t_k)] + (t - t_k)\cdot[\dot{R}_{x,i}\,(t)] \tag{11}$$

and

$$[y_j\,(t)] := y_{app,j}\,(t_k) + (t - t_k)\cdot\dot{y}_{app,j}\,(t_k) + [R_{y,j}\,(t)] \tag{12}$$

with $i = 1, \ldots, n_x$, $j = 1, \ldots, n_y$, and $t \in [t_k\ ;\ t_{k+1}]$, $t_0 \le t \le t_f$.

In (11) and (12), t_k and t_{k+1} are two subsequent points of time between which guaranteed state enclosures are determined. For $t = t_0$, the conditions

$$[x(t_0)] = x_{app}(t_0) + [R_x(t_0)] \tag{13}$$

and

$$[y(t_0)] = y_{app}(t_0) + [R_y(t_0)] \tag{14}$$

have to be fulfilled with approximate solutions $x_{app}(t)$ and $y_{app}(t)$. They are computed, for example, by the non-verified DAE solver DAETS [19–22].

The following three-stage algorithm allows us to determine guaranteed state enclosures of a system of DAEs using the Krawczyk iteration [13] which solves nonlinear algebraic equations in a verified way.

Step 1. Compute hidden constraints that have to be fulfilled for the verified enclosures of the initial conditions $x(0)$ and $y(0)$ as well as for the time responses $x(t)$ and $y(t)$ by considering algebraic equations $g_i(x)$ which do not depend explicitly on y. Differentiation with respect to time leads to

$$\frac{d^j g_i(x)}{dt^j} = \left(\frac{\partial L_f^{j-1} g_i(x)}{\partial x}\right)^T \cdot f(x,y) = L_f^j g_i(x) = 0 \tag{15}$$

with $L_f^0 g_i(x) = g_i(x)$. The Lie derivatives $L_f^j g_i(x)$ are computed automatically by using FADBAD++ [2] up to the smallest order $j > 0$ for which $L_f^j g_i(x)$ depends on at least one component of y.

Step 2. Compute initial conditions for the equations (9) and (10) such that the constraints (10) and (15) are fulfilled using the Krawczyk iteration.

Step 3. Substitute the state enclosures (11) and (12) for the vectors $x(t)$ and $y(t)$ in (9) and (10) and solve the resulting equations for $[\dot{R}_x(t)]$ and $[R_y(t)]$ with the help of the Krawczyk iteration. The hidden constraints (15) are employed to restrict the set of feasible solutions.

4 DAEs for Verified Feedforward Control and State Estimation

Besides simulation of systems with known control inputs, ValEncIA-IVP can be employed for *trajectory planning* and computation of *feedforward control* strategies for ODE and DAE systems. In the case of trajectory planning, reference signals $w(t)$ of open-loop controllers (S is open in Fig. 1) or closed-loop controllers (S is closed in Fig. 1) are calculated in such a way that the output $y(t)$ follows a desired time response $y_d(t)$ within given tolerances. For closed-loop control, the structure and parameters of $u(\hat{x}, w)$ are assumed to be determined beforehand using classical techniques for control synthesis.

State estimation techniques can be employed in the closed loop in Fig. 1 to reconstruct non-measured components of x_s, p, and q. The corresponding estimates $\hat{x}$ are then fed back as a substitute for the unknown quantities in the

closed-loop control $u(\hat{x}, w)$. In Fig. 1, the vectors p and q contain uncertainties of system parameters as well as interval bounds for measurement tolerances and errors.

To determine feedforward control strategies (and reference signals), we compute the inputs $u(t)$ (and $w(t)$) as components of the vector $y(t)$ of algebraic state variables in the DAEs (9),(10) after describing the desired system outputs by additional algebraic equations

$$0 = h(x_s(t), u(t), q(t), t) - (y_d(t) + y_{tol}(t)) \quad . \tag{16}$$

In these constraints, $[y_{tol}(t)]$ represents worst-case interval bounds for the tolerances $y_{tol}(t)$ between the actual and desired outputs $y(t)$ and $y_d(t)$. The resulting DAE system is solved by ValEncIA-IVP for the control sequence $u(t)$ and the consistent state trajectories $x(t)$.

Compared with approaches based on symbolic formula manipulation which can be applied to feedforward control of nonlinear exactly input-to-state linearizable sets of ODEs (as a special case of differentially flat systems) [5, 16], numerical interval-based approaches are more flexible. First, uncertainties and robustness requirements can be expressed directly in the constraints (16). In addition, the verified approach can also handle differentially non-flat systems if stability of the internal dynamics can be guaranteed [4, 32]. A short summary of verified stability analysis is also given in Section 5. For most of these non-flat systems, the output $y(t)$ does not coincide exactly with $y_d(t)$. However, verified techniques still allow us to compute control sequences (if they exist) for which the tolerances $[y_{tol}(t)] \neq [0\ ;\ 0]$ in (16) are not violated.

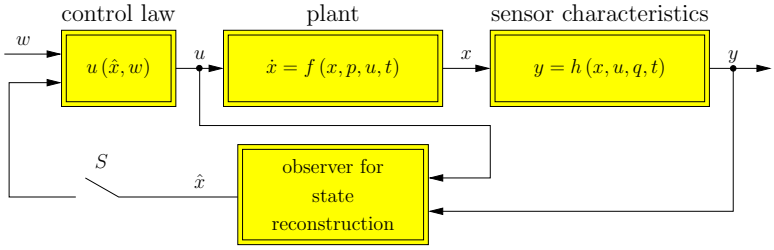

Fig. 1: Observer-based closed-loop control of nonlinear dynamical systems.

Since most control structures rely on information about *estimates* for non-measured states, parameters, and disturbances, the DAE approach has to be extended. In classical interval observers, a two-stage method is used. First, the non-measured quantities are reconstructed in a filter step by solving the measurement equations for the same number of variables as linearly independent measurements (cf. [11]). In a second stage, this estimate is predicted over time with the techniques from Sections 2 and 3 up to the point at which the next measured data are available.

In contrast, we can use the DAE-based solution procedure to implement a one-stage approach. To estimate the non-measured quantities, the equation

$$\begin{aligned} q(x) &= \left[y_m^T \; \dot{y}_m^T \; \ldots \; {y_m^{(n_x-1)}}^T \right]^T \\ &= \left[h(x)^T \; L_f h(x)^T \; \ldots \; L_f^{(n_x-1)} h(x)^T \right]^T \end{aligned} \tag{17}$$

describing the measured variables $y_m(t)$ and their i-th derivatives $y_m^{(i)}(t)$ has to be solved for the state vector $x(t) \in \mathbb{R}^{n_x}$.

In (17), $y_m^{(i)}(t)$ is expressed as the Lie derivative

$$L_f^i h(x) = L_f \left(L_f^{i-1} h(x) \right) \;\; , \;\; i = 0, \ldots, n_x - 1 \;\; , \tag{18}$$

of the output $h(x)$ along the vector field $f(x)$ with

$$L_f^0 h(x) = h(x) \quad \text{and} \quad L_f h(x) = \frac{\partial}{\partial x} h(x) \cdot f(x) \;\; . \tag{19}$$

The equation (17) can be solved (at least locally) for x, if the observability matrix

$$Q(x) = \left[Q_0^T(x) \; Q_1^T(x) \ldots Q_{n_x-1}^T(x) \right]^T \tag{20}$$

with $Q_i(x) = \frac{\partial}{\partial x} L_f^i h(x)$, corresponding to the Jacobian of $q(x)$ with respect to the state vector x, has the full rank n_x. The rank of $Q(x)$ yields sufficient information about the dimension of the observable manifold of the dynamical system [29, 32].

In ValEncIA-IVP, this functionality is implemented with the help of algorithmic differentiation, that is, without computation of the derivatives in (17)–(20) using symbolic formula manipulation.

For state, parameter, and disturbance estimation, the system's output equation $y_m(t) = h(x(t))$ is included in the interval-based DAE solver as a further time-dependent algebraic constraint with interval uncertainties of the measured variables and their derivatives. In that way, the Lie derivatives required in (17) coincide directly with the hidden constraints (15). These constraints are evaluated in each time interval in which ValEncIA-IVP is used to integrate the dynamical system model by solving the corresponding IVP. Therefore, the influence of measurement uncertainties on the quality of state estimates can be quantified directly by determining guaranteed consistent state enclosures.

Asymptotic stability of nonlinear closed-loop systems is not guaranteed if — as is usually the case — controllers and state estimators are parameterized independently. The procedures described in the following section should be applied to prove stability and to identify regions of attraction of (asymptotically) stable equilibria in a rigorous way.

5 Verified Stability Analysis of Uncertain Systems

For nonlinear dynamical systems, Lyapunov functions provide a suitable means for the numerical and — in special cases — analytical proof of asymptotic stabil-

ity. In general, both nominal system models and system models with parameter uncertainties can be considered.

The following verified approach for stability analysis relies on the selection of positive-definite candidates $V(x,p)$ for suitable Lyapunov functions.

An equilibrium x_∞ of a nonlinear dynamical system

$$\dot{x}(t) = f(x(t), p, u, t) \tag{21}$$

is *stable*, if a continuously differentiable function $V(x,p) : D \mapsto \mathbb{R}$ with

$$\begin{aligned} &V(x,p) = 0 \quad \text{for } x = x_\infty \ , \\ &V(x,p) > 0 \quad \text{for } x \neq x_\infty \ , \quad \text{and} \\ &\dot{V}(x,p) \leq 0 \quad \text{for } x \neq x_\infty \end{aligned} \tag{22}$$

exists. The equilibrium x_∞ of the dynamical system (21) is characterized by

$$f(x_\infty, p, u, t) = 0 \quad \text{with} \quad \frac{\partial f}{\partial t} = 0 \ , \tag{23}$$

where $u = u(x_\infty) = u_\infty = \text{const}$ and $p = p_\infty = \text{const}$ hold. The validity of the stability criterion (22) must be guaranteed in a neighborhood of the equilibrium x_∞. A dynamical system is globally stable if (22) holds for all $x \in \mathbb{R}^{n_x}$ (assuming that V is radially unbounded).

If the derivative with respect to time of the function $V(\cdot)$ in (22) can be proven to be negative definite instead of negative semi-definite along the trajectories of the dynamical system, it is *asymptotically stable* in a neighborhood of the equilibrium [10, 16]. Furthermore, using these conditions, we can often identify domains in the state-space which belong to the *region of attraction* of asymptotically stable equilibria [16].

Using interval arithmetic techniques, two different approaches for the verification of stability properties of nonlinear dynamical systems can be distinguished:

- Stability analysis based on interval evaluation of the above-mentioned Lyapunov functions and
- Tests for convergence of guaranteed enclosures of the sets of all reachable states over time towards an equilibrium.

Before we can apply these approaches, a guaranteed enclosure $[x_\infty]$ of the unique equilibrium x_∞ has to be computed using, for example, interval Newton techniques. If the dynamical system model depends on interval parameters $p \in [p]$, the equilibrium is usually parameter dependent. Then, the set of all possible equilibria has to be included within the box $[x_\infty]$. For simplicity, only time-invariant dynamical systems are considered in the following.

5.1 Stability Analysis Using Interval Evaluation of Lyapunov Functions

The following description of interval-based stability analysis using Lyapunov functions is based on [4]. Having computed the interval enclosure $[x_\infty]$, we choose

a double-valued approximate solution $\tilde{x}_\infty \in [x_\infty]$. Then, an approximation A of the system's Jacobian is determined for $\tilde{x}_\infty$ according to

$$A := \left.\frac{\partial f}{\partial x}\right|_{x=\tilde{x}_\infty} . \tag{24}$$

With this matrix, the Lyapunov equation

$$A^T P + PA = -I \tag{25}$$

of the linearized system is solved for the symmetric matrix P. Using this approach, stability analysis of the linearized system model is considered in a first stage to derive a suitable candidate for a quadratic Lyapunov function. If the matrix P is positive definite, that is, if the linearized system can be proven to be asymptotically stable, an estimate for the region of attraction of an asymptotically stable equilibrium of the original nonlinear system can be determined.

For that purpose, an interval box $[x_0]$ for which $[x_\infty] \subset [x_0]$ holds is chosen. Additionally, this box must not contain further equilibria. Therefore, the initialization of the interval Newton iteration used to determine $[x_\infty]$ is typically chosen.

To analyze the stability of the dynamical system, the quadratic Lyapunov function

$$V(x,p) = (x - x_\infty)^T \cdot P \cdot (x - x_\infty) \tag{26}$$

with P determined in (25) is used. For the time derivative of this Lyapunov function, the properties

$$\dot{V}(x,p)\Big|_{x=x_\infty} = 0 \quad \text{and} \quad \left.\frac{\partial \dot{V}(x,p)}{\partial x}\right|_{x=x_\infty} = 0 \tag{27}$$

hold. Then, the Hessian

$$H := -\frac{\partial^2 \dot{V}(x,p)}{\partial x^2} \tag{28}$$

has to be shown to be positive definite for all $x \in [x_0]$. This can be done using a procedure described in [34].

A symmetric interval matrix

$$[H] = \{\, H \,|\, H_c - \Delta \leq H \leq H_c + \Delta \} \tag{29}$$

with

$$H_c = \tfrac{1}{2}\left(\underline{H} + \overline{H}\right) \qquad \text{and} \qquad \Delta = \tfrac{1}{2}\left(\overline{H} - \underline{H}\right) \tag{30}$$

is positive definite if the following $2^{n_x - 1}$ point matrices $H_z = H_{-z}$ are positive definite. The matrices H_z are defined according to

$$H_z := H_c - T_z \cdot \Delta \cdot T_z \qquad \text{with} \qquad T_z := \operatorname{diag}\{(z)\} \quad . \tag{31}$$

The vector z has to be replaced by all possible combinations of the components $z_i = \pm 1$, $i = 1, \ldots, n_x$. Thus, $H_z = H_{-z}$ holds.

As shown in [4], the interval box $[x]$ with center in $[x_\infty]$ and radius

$$\sqrt{n_x \frac{\lambda_{\min}}{\lambda_{\max}}}\, d\left([x_\infty], [x_0]\right) \tag{32}$$

certainly belongs to the region of attraction of an *asymptotically stable* equilibrium x_∞. In (32), $\lambda_{\min}$ and $\lambda_{\max}$ are the minimum and maximum eigenvalues of P, respectively. Furthermore, d is a function defined on $\mathbb{IR}^{n_x} \times \mathbb{IR}^{n_x}$ with

$$d : ([x], [y]) \mapsto \sup \{ r \in \mathbb{R} | \, B(r, [x]) \subset [y] \} \quad , \tag{33}$$

an interval box $[x] \subset \mathbb{IR}^{n_x}$, and $B(r, [x])$ denoting the set

$$\left\{ x \in \mathbb{R}^{n_x} \middle| \min_{a \in [x]} \|a - x\| < r \right\} \quad . \tag{34}$$

5.2 Stability Analysis by Propagation of Guaranteed State Enclosures

In addition to stability analysis using Lyapunov functions, the computation of guaranteed state enclosures can also be used to determine interval boxes included in the regions of attraction of *stable* equilibria. For that purpose, the set of all reachable states is computed, starting from an interval box $[x_0]$ at a point of time $t = t_1$, see left hand side of Fig. 2.

If it can be shown that the set of reachable states at a point of time $t_2 > t_1$ is included completely in the interior of $[x_0]$, the stability of the dynamical system is proven under the condition that the mathematical system model does not explicitly depend on time. On the right hand side of Fig. 2, a typical result is shown. In order to identify stability, we often have to split interval enclosures into smaller subdomains. The result of propagation of these subintervals is illustrated by gray boxes in Fig 2.

Note that due to overestimation which often occurs in interval evaluation of dynamical system models, both approaches for the verification of stability properties are only sufficient criteria. If one of these methods fails to verify (asymptotic) stability, we either have to prove instability or exploit further techniques for reduction of overestimation, that is, for computation of tighter interval bounds.

Example 5.1 Consider the nonlinear system

$$\dot{x}(t) = a x^3(t) + u(t) \tag{35}$$

with the given linear feedback control structure

$$u(t) = -k x(t) \tag{36}$$

and the uncertain parameter $a \in [\underline{a} \, ; \, \overline{a}]$. Using the verified approach for stability analysis, the candidate for a Lyapunov function

$$V = x^2 \tag{37}$$

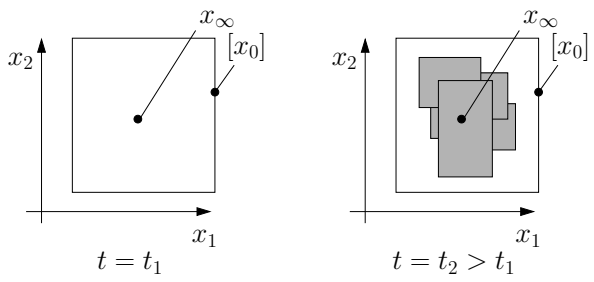

Fig. 2: Stability analysis of nonlinear dynamical systems using verified integration of ODEs.

is obtained if the equilibrium $x_\infty = 0$ is checked for stability. After computation of its derivative

$$\dot{V} = 2ax^4 - kx^2 \tag{38}$$

one obtains

$$H = -\frac{\partial^2 \dot{V}}{\partial x^2} = -24ax^2 + 4k \overset{!}{>} 0 \quad \text{for all} \quad a \in [a] \ , x \in [x] \tag{39}$$

as the prerequisite for the guaranteed domain of attraction of the stable equilibrium. This means that

$$k > 6ax^2 \tag{40}$$

must hold for all $a \in [a]$ if $x \in [x]$ is the desired region of attraction, corresponding to

$$k > 6\overline{a} \max\left\{\underline{x}^2; \overline{x}^2\right\} \ . \tag{41}$$

■

Example 5.2 Now, stability of the uncertain system

$$\dot{x}(t) = -x^3(t) + p \ , \quad p \in [p] \ , \quad \underline{p} > 0 \tag{42}$$

with the interval enclosure $[x_\infty] = \sqrt[3]{[p]}$ of its equilibria is analyzed. For this system,

$$V = (x - [x_\infty])^2 = (x - \sqrt[3]{p})^2 \ , \quad p \in [p] \tag{43}$$

and

$$\dot{V} = -x^4 + px + \sqrt[3]{p}x^3 - p\sqrt[3]{p} \ , \quad p \in [p] \tag{44}$$

hold if p is a constant but uncertain parameter. Again, positivity of

$$H = 12x^2 - 6\sqrt[3]{p}x \overset{!}{>} 0 \ , \quad p \in [p] \tag{45}$$

has to be verified leading to the set

$$x > \frac{1}{2}\sqrt[3]{\overline{p}} \tag{46}$$

as the guaranteed region of attraction of the stable equilibria $[x_\infty]$. Note that this is only a conservative condition since $\dot{V}$ in (44) is negative definite for all $x \in \mathbb{R}$ and all $p \in [p] = \text{const} > 0$, meaning that all equilibria are globally asymptotically stable. ■

6 Control of a Distributed Heating System

6.1 Basic Experimental Setup

To visualize the practical applicability of verified DAE solvers for feedforward control as well as state and disturbance estimation, we consider the distributed heating system in Fig. 3. The controlled variable of this system is the temperature at a given position of the rod. Control and disturbance inputs are provided by four Peltier elements and cooling units. The temperature $\vartheta(z,t)$ of the rod depends both on the spatial variable z and on the time t.

Mathematically, the temperature distribution is given by the parabolic PDE

$$\frac{\partial\vartheta(z,t)}{\partial t} - \frac{\lambda}{\rho c_p}\frac{\partial^2\vartheta(z,t)}{\partial z^2} + \frac{\alpha}{h\rho c_p}\vartheta(z,t) = \frac{\alpha}{h\rho c_p}\vartheta_U \tag{47}$$

which is discretized in its spatial coordinate into finite volume elements to obtain a model for offline simulation as well as for online state and disturbance estimation. Balancing of heat exchange between four volume elements leads to the ODEs

$$\begin{bmatrix}\dot{x}_1(t)\\ \dot{x}_2(t)\\ \dot{x}_3(t)\\ \dot{x}_4(t)\end{bmatrix} = \begin{bmatrix}a_{11} & a_{12} & 0 & 0\\ a_{12} & a_{22} & a_{12} & 0\\ 0 & a_{12} & a_{22} & a_{12}\\ 0 & 0 & a_{12} & a_{11}\end{bmatrix} \cdot \begin{bmatrix}x_1(t)\\ x_2(t)\\ x_3(t)\\ x_4(t)\end{bmatrix} + \frac{1}{m_s c_p}\begin{bmatrix}1\\0\\0\\0\end{bmatrix} u(t) + \frac{\alpha A}{m_s c_p}\begin{bmatrix}e_1(t)\\ e_2(t)\\ e_3(t)\\ e_4(t)\end{bmatrix} \tag{48}$$

for the temperatures $x_i(t)$ in the segments $i = 1, \ldots, n = 4$ with the coefficients

$$a_{11} = -\frac{\alpha A l_s + \lambda_s b h}{l_s m_s c_p}\ , \quad a_{12} = \frac{\lambda_s b h}{l_s m_s c_p}\ , \quad \text{and} \quad a_{22} = -\frac{\alpha A l_s + 2\lambda_s b h}{l_s m_s c_p}\ . \tag{49}$$

In (48), the input signal $u(t)$ corresponds to the heat flow into the first segment of the rod. The goal of feedforward control (determined by ValEncIA-IVP or DAETS) is the computation of an input $u(t) = u_1(t)$ in such a way that the output temperature $y(t)$ in an arbitrary segment tracks the desired temperature profile

$$y_d(t) = \vartheta_0 + \frac{(\vartheta_f - \vartheta_0)}{2}\left(1 + \tanh\left(k\left(t - \frac{3600\,\text{s}}{2}\right)\right)\right) \tag{50}$$

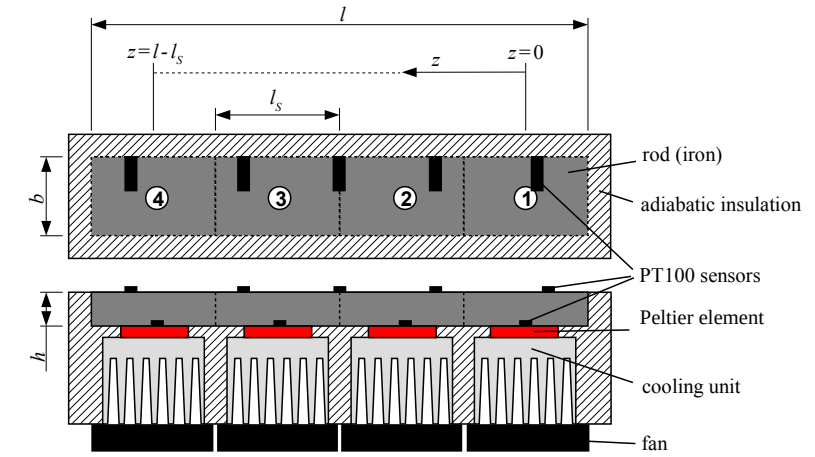

$\rho = 7800$ kg/m^3	density of iron	$b = 40$ mm	width of the rod
$c_p = 420$ J/(kg·K)	specific heat capacity	$h = 12$ mm	height of the rod
$\lambda = 110$ W/(m·K)	heat conductance	m_S	mass of segment
$\alpha = 50$ W/(m^2·K)	heat transfer coefficient	$\vartheta_U = 293.15$ K	ambient temperature
$l = 320$ mm	total length of the rod		(for simulation/ measured at $t = 0$ in experiment)
$l_s = l/n$	length of segment	$\vartheta(z,t)$	temperature profile
$n = 4$	number of segments	x_i	temperature in i-th segment

Fig. 3: Experimental setup of a distributed heating system.

with $\vartheta_0 = \vartheta_U(0)$, $\vartheta_f = \vartheta_0 + 10\,\mathrm{K}$, and $k = 0.0015$ exactly. The prediction time horizon for the DAE solver is $t_{k+1} - t_k = 1\,\mathrm{s}$. For defuzzification of the control intervals, the definition $u_1(t) = 0.5 \cdot (\underline{u}_1(t) + \overline{u}_1(t))$ with $t \in [t_k; t_{k+1})$ is used.

The additive terms $e_i(t)$, $i = 1, \ldots, n = 4$ summarize errors resulting from the discretization of the PDE and unmodeled disturbances which are estimated by a Luenberger observer and the novel DAE-based approach, see the experimental results in Fig. 4. The interval observer detects the point of time from which on the Luenberger observer yields consistent estimates. Both estimators make use of the measured temperatures $y_1 = x_1$ and $y_2 = x_4$. If model errors are neglected, all e_i are equal to the ambient temperature $\vartheta_U(0)$.

For the implementation of the disturbance observer, the ODEs (48) are extended by $\dot{e} = 0$ with $e = e_1 = \ldots = e_4$. To quantify the influence of measurement errors, the uncertainties $x_i \in y_j + [-1\ ;\ 1]\,\mathrm{K}$, $\dot{x}_i \in [-0.5\ ;\ 1.5]\,\dot{y}_j$, $i \in \{1, 4\}$, $j \in \{1, 2\}$ are considered in the DAE-based estimator. To compensate model errors and disturbances, output feedback $u_2(t)$ is introduced in addition to the feedforward control $u_1(t)$ by a PI controller

$$u_2(t) = K_I \cdot \left((y_d(t) - y(t)) + \frac{1}{T_I} \int_0^t (y_d(\tau) - y(\tau))\, d\tau \right) \tag{51}$$

with $K_I = 3$ and $T_I = 786\,\mathrm{s}$ compensating the largest time constant T_I of the plant (48). Therefore, the total control input is given by $u\,(t) = u_1\,(t) + u_2\,(t)$.

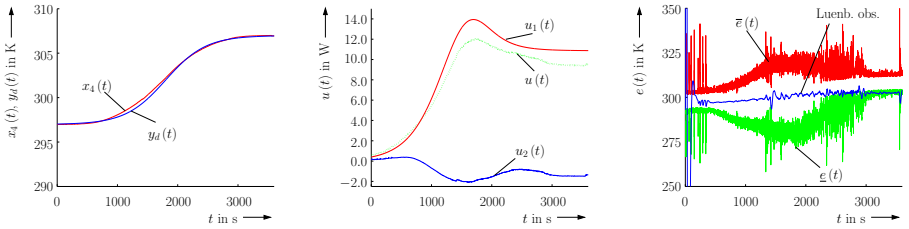

(a) Output temperature $x_4\,(t)$. (b) Control variable $u\,(t)$. (c) Disturbance estimate $e\,(t)$.

Fig. 4: Experimental results for closed-loop control of the heating system.

6.2 Structural Analysis for Specification of Flat Outputs

For specification of the flat output

$$g\,(x,t) = x_4\,(t) - y_d\,(t) = 0 \tag{52}$$

of the system, the same state equations as in Subsection 6.1 are considered with the assumption that the error terms $e_i\,(t)$ are piecewise constant. In this case, the structural analysis performed in ValEncIA-IVP provides the following result:

	x_1	x_2	x_3	x_4	t	u
$\dot{x}_1$	•	•				•
$\dot{x}_2$	•	•	•			
$\dot{x}_3$		•	•	◇		
$\dot{x}_4$			•	◇		
$g(x,t)$				◇	◇	

	x_1	x_2	x_3	x_4	t	u
$L_f^0 g$				◇	◇	
$L_f^1 g$			•	◇	◇	
$L_f^2 g$		•	•	◇	◇	
$L_f^3 g$	•	•	•	◇	◇	
$L_f^4 g$	•	•	•	◇	◇	•

Legend:

◇	a-priori known
•	determined via algebraic constraints of the DAE system

The Lie derivative $L_f^4 g$ corresponds to the smallest order of the derivative of the output equation $g\,(x,t)$ which is influenced directly by the control input u. Since the number of unknowns (all unknowns are marked by • in the previous scheme) and the number of hidden constraints are identical in this case, the

equations $L_f^1 g = 0, \ldots, L_f^4 g = 0$ can be solved directly by application of interval Newton techniques for the consistent states x_1, x_2, and x_3, as well as the desired control input u. Since all internal states x_i, $i = 1, \ldots, 4$, and the control u are uniquely defined by y_d and a finite number of its derivatives, the output $y = x_4$ corresponds to the system's flat output. Note that the value of x_4 is known a-priori by evaluation of $g = L_f^0 g = 0$ for each point of time t, which is denoted by $\diamond$. In the case described in this subsection, the solution is uniquely defined by specification of the desired system output. That is, besides specification of the output profile in (52), no additional initial conditions are required for the synthesis of the corresponding feedforward control. However, this also means that deviations of the initial temperature distribution in the rod from the values specified by the equations $L_f^1 g = 0, \ldots, L_f^4 g = 0$ inevitably lead to tracking errors $y(t) - y_d(t) \neq 0$. These deviations can be compensated by output feedback controllers according to Subsection 6.1.

As an alternative to the interval-based computation of feedforward control using ValEncIA-IVP (and its structural analysis which allows us to determine guaranteed enclosures of all admissible initial conditions in a given domain), the non-verified solver DAETS can be used if no interval uncertainties are considered for parameters and modeling errors. In Fig. 5, the control inputs $u(t)$ are displayed which lead to the output defined in (52). For the visualization without interval uncertainties, the non-verified DAE solver DAETS has been used to determined the feedforward control for different variations $\Delta\vartheta = \vartheta_f - \vartheta_0$ of the output temperature as well as for different values of k influencing the slope of $y_d(t)$ in the transient phase.

6.3 Structural Analysis for Specification of Non-Flat Outputs

For specification of a non-flat output, for example

$$g(x,t) = x_3(t) - y_d(t) = 0 \ , \tag{53}$$

the order δ of the derivative of the output equation g which is influenced directly by the control input u is smaller than the number of unknown variables. For that reason, the relative degree δ of the system is smaller than the dimension of the state vector.

Since the number of unknowns is now larger than the number of hidden constraints, the equations $L_f^1 g = 0, \ldots, L_f^\delta g = 0$ cannot be solved directly by application of interval Newton techniques to obtain the missing consistent states (denoted by $\bullet$) and the desired control input u. This is also demonstrated by the following result of the structural analysis.

	x_1	x_2	x_3	x_4	t	u
$\dot{x}_1$	$\bullet$	$\bullet$				$\bullet$
$\dot{x}_2$	$\bullet$	$\bullet$	$\diamond$			
$\dot{x}_3$		$\bullet$	$\diamond$	$\bullet$		
$\dot{x}_4$			$\diamond$	$\bullet$		
$g(x,t)$			$\diamond$		$\diamond$	

	x_1	x_2	x_3	x_4	t	u
$L_f^0 g$			$\diamond$		$\diamond$	
$L_f^1 g$		$\bullet$	$\diamond$	$\bullet$	$\diamond$	
$L_f^2 g$	$\bullet$	$\bullet$	$\diamond$	$\bullet$	$\diamond$	
$L_f^3 g$	$\bullet$	$\bullet$	$\diamond$	$\bullet$	$\diamond$	$\bullet$

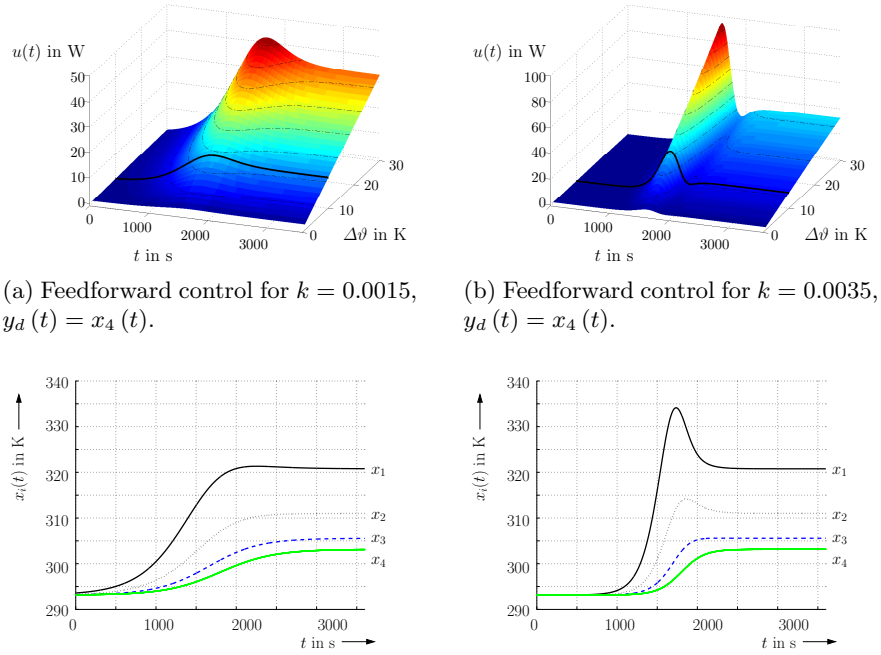

(a) Feedforward control for $k = 0.0015$, $y_d\,(t) = x_4\,(t)$.

(b) Feedforward control for $k = 0.0035$, $y_d\,(t) = x_4\,(t)$.

(c) Feedforward control for $k = 0.0015$, $y_d\,(t) = x_4\,(t)$.

(d) Feedforward control for $k = 0.0035$, $y_d\,(t) = x_4\,(t)$.

Fig. 5: Feedforward control for specification of the flat output $x_4\,(t)$.

Therefore, to solve this system, further information about the initial conditions has to be taken into account in the following two-stage procedure. In the first stage, we identify a set of ODEs or DAEs which includes the system's output and can be solved as an IVP by specification of a suitable number of initial conditions. The resulting equations describe either an IVP for ODEs or an IVP for a set of DAEs. In the first case, all initial conditions can be specified arbitrarily. In the second case, the initial conditions have to be computed consistently with the help of the output equation $g = L_f^0 g = 0$ and, if necessary, the lower-order constraints $L_f^1 g = 0, \ldots, L_f^\tau g = 0$, $\tau < \delta$. In the second stage, this solution to the IVP is substituted for the corresponding state variables (denoted by $\circ$) in $L_f^{\tau+1} g = 0, \ldots, L_f^\delta g = 0$. These equations, which are purely algebraic, are now solved for the remaining states (denoted by $\bullet$) and the control input $u\,(t)$ using interval Newton techniques.

In the following, this procedure is demonstrated for the system model (48) and the output specification (53). For specification of x_3 as the desired output (denoted by $\diamond$), it is at least necessary to know the initial temperature $x_4(0)$. Then, an IVP for the ODE for $x_4\,(t)$ is solved in the first stage with the known

temperature profile $x_3(t)$. This information is substituted for $x_4(t)$ in the constraints $L_f^1 g = 0, \ldots, L_f^\delta g = 0$, which can now be solved for the remaining unknowns.

	x_1	x_2	x_3	x_4	t	u
$\dot{x}_1$	●	●				●
$\dot{x}_2$	●	●	◇			
$\dot{x}_3$		●	◇	○		
$\dot{x}_4$			◇	○		
$g(x,t)$			◇		◇	

	x_1	x_2	x_3	x_4	t	u
$L_f^0 g$			◇		◇	
$L_f^1 g$		●	◇	○	◇	
$L_f^2 g$	●	●	◇	○	◇	
$L_f^3 g$	●	●	◇	○	◇	●

Alternatively, the solution of IVPs using a DAE solver with the given initial conditions $x_2(0)$, $x_4(0)$, and the constraint $L_f^1 g = 0$ (or the initial conditions $x_1(0), x_2(0), x_4(0)$, and the constraints $L_f^1 g = 0$, $L_f^2 g = 0$, respectively) produces the same result. The variables which are determined by the verified DAE solver in this first stage are denoted by $*$ in the following schemes. The remaining constraints $L_f^2 g = 0$, $L_f^3 g = 0$ (or only $L_f^3 g = 0$, respectively), are used to compute the consistent internal system states and the input u in the stage 2 of the solution approach, denoted again by ●.

	x_1	x_2	x_3	x_4	t	u
$\dot{x}_1$	●	$*$				●
$\dot{x}_2$	●	$*$	◇			
$\dot{x}_3$		$*$	◇	○		
$\dot{x}_4$			◇	○		
$g(x,t)$			◇		◇	

	x_1	x_2	x_3	x_4	t	u
$L_f^0 g$			◇		◇	
$L_f^1 g$		$*$	◇	○	◇	
$L_f^2 g$	●	$*$	◇	○	◇	
$L_f^3 g$	●	$*$	◇	○	◇	●

	x_1	x_2	x_3	x_4	t	u
$\dot{x}_1$	$*$	○				●
$\dot{x}_2$	$*$	○	◇			
$\dot{x}_3$		○	◇	○		
$\dot{x}_4$			◇	○		
$g(x,t)$			◇		◇	

	x_1	x_2	x_3	x_4	t	u
$L_f^0 g$			◇		◇	
$L_f^1 g$		○	◇	○	◇	
$L_f^2 g$	$*$	○	◇	○	◇	
$L_f^3 g$	$*$	○	◇	○	◇	●

Legend:

◇	a-priori known
○	determined via IVP solver (ODE/ DAE)
$*$	determined via algebraic constraints of DAE (stage 1) (not required if the flat output is specified directly)
●	determined via algebraic constraints of DAE (stage 2)

In analogy to the specification of the flat system output, the non-verified solver DAETS is applied as an alternative solution procedure. In Fig. 6, the corresponding control inputs (as feedforward control sequence) are displayed for the non-flat case if x_3 is specified by the function (50) as the system output. For the visualization by DAETS, the feedforward control is determined for different variations $\Delta\vartheta = \vartheta_f - \vartheta_0$ of the output temperature and different values of k.

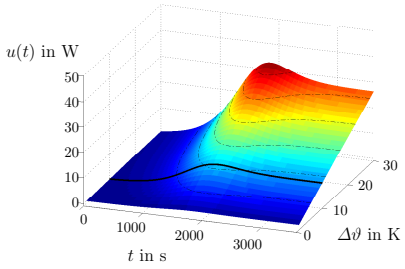

(a) Feedforward control for $k = 0.0015$, $y_d\,(t) = x_3\,(t)$.

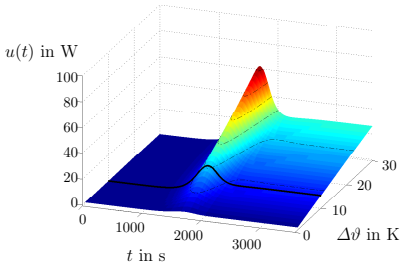

(b) Feedforward control for $k = 0.0035$, $y_d\,(t) = x_3\,(t)$.

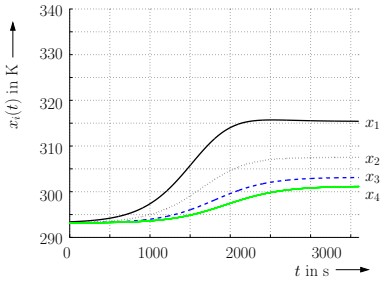

(c) Feedforward control for $k = 0.0015$, $y_d\,(t) = x_3\,(t)$.

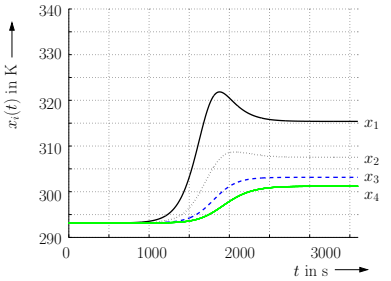

(d) Feedforward control for $k = 0.0035$, $y_d\,(t) = x_3\,(t)$.

Fig. 6: Feedforward control for specification of the non-flat output $x_3\,(t)$.

7 Extended Experimental Setup of the Distributed Heating System

7.1 Derivation of a Control-Oriented Model

After extending the experimental setup depicted in Fig. 3 by an air canal on top of the metallic rod, we can formulate a new control task: Control the mass flow of air in the canal by adjusting the speed of a corresponding fan so that the temperature in the metallic rod does not exceed a predefined maximum value.

For that purpose, a first simple finite-dimensional model can be identified to approximate the dynamics of the temperature distribution in the rod and in the air canal similarly to the finite volume model in (48). If the volume of the air canal is discretized into the same number of segments as the rod, we obtain the

ODEs

$$
\begin{aligned}
\dot{\vartheta}_1 &= \frac{1}{\rho_S c_S V_{SE}} \left[\dot{Q}_{H1} - \frac{\lambda_S A_{Sq}}{l_{SE}} (\vartheta_1 - \vartheta_2) - \alpha_S A_{SE} (\vartheta_1 - \vartheta_8) \right] \\
\dot{\vartheta}_2 &= \frac{1}{\rho_S c_S V_{SE}} \left[\dot{Q}_{H2} + \frac{\lambda_S A_{Sq}}{l_{SE}} (\vartheta_1 - \vartheta_2) - \frac{\lambda_S A_{Sq}}{l_{SE}} (\vartheta_2 - \vartheta_3) - \alpha_S A_{SE} (\vartheta_2 - \vartheta_7) \right] \\
\dot{\vartheta}_3 &= \frac{1}{\rho_S c_S V_{SE}} \left[\dot{Q}_{H3} + \frac{\lambda_S A_{Sq}}{l_{SE}} (\vartheta_2 - \vartheta_3) - \frac{\lambda_S A_{Sq}}{l_{SE}} (\vartheta_3 - \vartheta_4) - \alpha_S A_{SE} (\vartheta_3 - \vartheta_6) \right] \\
\dot{\vartheta}_4 &= \frac{1}{\rho_S c_S V_{SE}} \left[\dot{Q}_{H4} + \frac{\lambda_S A_{Sq}}{l_{SE}} (\vartheta_3 - \vartheta_4) - \alpha_S A_{SE} (\vartheta_4 - \vartheta_5) \right] \\
\dot{\vartheta}_5 &= \frac{1}{\rho_L c_L V_{LE}} \left[\dot{m} c_L (\vartheta_6 - \vartheta_5) - \alpha_L A_{LE} (\vartheta_5 - \vartheta_U) + \alpha_S A_{SE} (\vartheta_4 - \vartheta_5) \right] \\
\dot{\vartheta}_6 &= \frac{1}{\rho_L c_L V_{LE}} \left[\dot{m} c_L (\vartheta_7 - \vartheta_6) - \alpha_L A_{LE} (\vartheta_6 - \vartheta_U) + \alpha_S A_{SE} (\vartheta_3 - \vartheta_6) \right] \\
\dot{\vartheta}_7 &= \frac{1}{\rho_L c_L V_{LE}} \left[\dot{m} c_L (\vartheta_8 - \vartheta_7) - \alpha_L A_{LE} (\vartheta_7 - \vartheta_U) + \alpha_S A_{SE} (\vartheta_2 - \vartheta_7) \right] \\
\dot{\vartheta}_8 &= \frac{1}{\rho_L c_L V_{LE}} \left[\dot{m} c_L (\vartheta_E - \vartheta_8) - \alpha_L A_{LE} (\vartheta_8 - \vartheta_U) + \alpha_S A_{SE} (\vartheta_1 - \vartheta_8) \right] \quad .
\end{aligned}
\tag{54}
$$

This model takes into account heat conduction in the metallic rod, convective heat transfer between the rod and the air canal, as well as between the air canal and the ambient air. Furthermore, the transport of air in the interior of the canal with different inlet and outlet temperatures is described under consideration of the specific heat capacity c_L of air and the corresponding mass flow $\dot{m}$.

In contrast to the previous setup in Fig. 3, the heat flow $\dot{Q}_{H1}, \ldots \dot{Q}_{H4}$ of the four Peltier elements does not serve as a control input but as a distributed disturbance to be compensated by variations of the mass flow $\dot{m}$. The compensation has to be performed in such a way that the maximum temperature in the interior of the rod does not exceed a predefined value. Since the position of this temperature is not a-priori known, it has to be determined with the help of suitable estimation strategies on the basis of the available measured data. In a first stage, the temperatures $\vartheta_1, \ldots, \vartheta_4$ in the four rod segments as well as the air temperature at the inlet and outlet segments of the air canal (ϑ_8 and ϑ_5, respectively) are measured.

The temperatures ϑ_i, $i = 5, \ldots, 8$, in the finite volume elements for the air canal are indexed such that the following rod and air canal segments are on top of each other: 1 and 8, 2 and 7, 3 and 6, 4 and 5. Moreover, the ambient air temperature is denoted by ϑ_U and the inlet temperature by ϑ_E.

According to Fig. 3, $V_{SE} = \frac{V_S}{4}$ denotes the volume of one segment in the rod (total volume V_S), $A_{SE} = \frac{A_S}{4}$ its surface (total surface A_S), $l_{SE} = \frac{l_S}{4}$ the length of one segment, A_{Sq} the area of the cross section of the rod, c_S its specific heat capacity, and ρ_S the density of iron. Similarly, the parameters for the air canal are defined, namely the volume of one element $V_{LE} = \frac{V_L}{4}$, its surface $A_{LE} = \frac{A_L}{4}$, the length of one segment $l_{LE} = \frac{l_L}{4}$, and its cross section A_{Lq}. The air stream is

parameterized by its specific heat capacity c_L, its density ρ_L, and the mass flow $\dot{m}$.

The remaining parameters are the coefficient for heat conduction λ_S in the rod, the convective heat transfer coefficients α_S and α_L between the rod and the air canal as well as between the air canal and the ambient air, respectively.

All geometric and physical parameters except for the effective values of the coefficients for convective and conductive heat transfer can be assumed to be independent of the mass flow $\dot{m}$. Therefore, they are known a-priori. In contrast, it is inevitable to identify the exact influence of the mass flow $\dot{m}$ on the parameters λ_S, α_S, and α_L experimentally, see the following subsection.

7.2 Model-Based Parameter Identification

To quantify the influence of $\dot{m}$ on the parameters λ_S, α_S, and α_L, the temperatures $\vartheta_1(t), \ldots, \vartheta_4(t)$ in the metallic rod as well as the temperatures $\vartheta_8(t)$,$\vartheta_5(t)$ in the inlet and outlet segments of the air canal were measured for known and constant $\dot{Q}_{H1}, \ldots, \dot{Q}_{H4}$ and variable $\dot{m}$, see Fig. 7.

Since no sensors are available in the experimental setup to determine the temperatures $\vartheta_6(t)$ and $\vartheta_7(t)$ directly, they are replaced by the following linear interpolation

$$\begin{aligned} \vartheta_6(t) &= \vartheta_5(t) + \frac{1}{3}\left(\vartheta_8(t) - \vartheta_5(t)\right) \quad \text{and} \\ \vartheta_7(t) &= \vartheta_5(t) + \frac{2}{3}\left(\vartheta_8(t) - \vartheta_5(t)\right) \end{aligned} \tag{55}$$

for the experimental identification of λ_S, α_S, and α_L.

In order to determine these parameters with the help of least-squares estimates, the state equations (54) are replaced by the state-space model

$$\begin{aligned} \dot{\vartheta}_1 &= K_1\dot{Q}_{H1} - p_1(\vartheta_1 - \vartheta_2) - p_2(\vartheta_1 - \vartheta_8) \\ \dot{\vartheta}_2 &= K_1\dot{Q}_{H2} + p_1(\vartheta_1 - \vartheta_2) - p_1(\vartheta_2 - \vartheta_3) - p_2(\vartheta_2 - \vartheta_7) \\ \dot{\vartheta}_3 &= K_1\dot{Q}_{H3} + p_1(\vartheta_2 - \vartheta_3) - p_1(\vartheta_3 - \vartheta_4) - p_2(\vartheta_3 - \vartheta_6) \\ \dot{\vartheta}_4 &= K_1\dot{Q}_{H4} + p_1(\vartheta_3 - \vartheta_4) - p_2(\vartheta_4 - \vartheta_5) \\ \dot{\vartheta}_5 &= p_3\dot{m}(\vartheta_6 - \vartheta_5) - p_4(\vartheta_5 - \vartheta_U) + p_5(\vartheta_4 - \vartheta_5) \\ \dot{\vartheta}_6 &= p_3\dot{m}(\vartheta_7 - \vartheta_6) - p_4(\vartheta_6 - \vartheta_U) + p_5(\vartheta_3 - \vartheta_6) \\ \dot{\vartheta}_7 &= p_3\dot{m}(\vartheta_8 - \vartheta_7) - p_4(\vartheta_7 - \vartheta_U) + p_5(\vartheta_2 - \vartheta_7) \\ \dot{\vartheta}_8 &= p_3\dot{m}(\vartheta_E - \vartheta_8) - p_4(\vartheta_8 - \vartheta_U) + p_5(\vartheta_1 - \vartheta_8) \quad . \end{aligned} \tag{56}$$

This modified system model depends linearly on the unknown coefficients p_1, p_2, p_4, and p_5. Therefore, these parameters can be identified easily by minimizing

the quadratic cost function

$$J = \sum_{k=1}^{M} \sum_{i \in \{1,2,3,4,5,8\}} \Big(\left(\vartheta_i\left(t_{k+1}\right) - \vartheta_i\left(t_k\right)\right) - T f_i\left(\vartheta_1\left(t_k\right), \ldots, \vartheta_8\left(t_k\right), \vartheta_E, \vartheta_U, p_1\left(\dot{m}\right), \ldots, p_5\left(\dot{m}\right), K_1\right) \Big)^2 . \tag{57}$$

Here, $T = 0.5\,\mathrm{s}$ denotes the sampling period between two subsequent measurements and f_i the i-th equation of the system model (56).

The cost function (57) has been minimized in usual floating point arithmetic. In compliance with theoretical results from physics, it could be shown in this identification that especially the parameters related to the air canal depend significantly on the mass flow $\dot{m}$, see also Fig. 8. For further stages in control design, these dependencies can be approximated using polynomials of the order 6.

The approximation quality obtained by this identification procedure can be checked by comparing the measured temperature profiles and the corresponding results for solution of an IVP (performed with a classical Runge-Kutta method) for the equations (56) with identical initial conditions, see Fig. 9. Note that the visible offset between measurements and simulations is mainly caused by errors in the temperatures of the ambient air and the inlet into the air canal. These temperatures ϑ_U and ϑ_E cannot be measured so far in the experiment and are therefore replaced by rough estimates. In an extension of the presented approach, it is possible either to include measurements of these values (after integration of further sensors in the setup) or to estimate these values by minimization of the deviation between experiment and simulations.

Future work for the design of controllers and verified models for the extended heating system will take into account verified least-squares estimates to determine the parameters p_1, p_2, p_4, and p_5. With their help, we can quantify estimation errors resulting from inaccurate measurements and spatial discretization errors in the replacement of the original infinite-dimensional model by the finite volume representations (54) and (56). For that purpose, additive disturbances can be considered similarly to the terms e_i in (48), see also [24].

Note that the direct computation of consistent state and control trajectories as discussed for the simple heating system in the Section 6, is very difficult for the extended setup if, for example, a desired profile is specified for one of the rod temperatures ϑ_i, $i = 1, \ldots, 4$. The reason for this is that the extended system model is no longer quasi-linear. Already the first derivatives of each of the rod temperatures depend on the control input $\dot{m}$ which has to determined if an open-loop or closed-loop control design is investigated. In the open-loop case, it is necessary to compute consistent trajectories of all internal system states ϑ_i, $i = 1, \ldots, 8$ in addition to $\dot{m}$ via hidden constraints (cf. Subsections 6.2 and 6.3). Since the system is no longer quasi-linear it is necessary to specify initial conditions for the remaining state variables and, additionally, for $\dot{m}$ and several of its derivatives.

This task will be dealt with in future work. Alternatively, it will be investigated how verified sensitivities $\frac{\partial \vartheta_i}{\partial \dot{m}}$ can be used to adapt the air mass flow $\dot{m}$

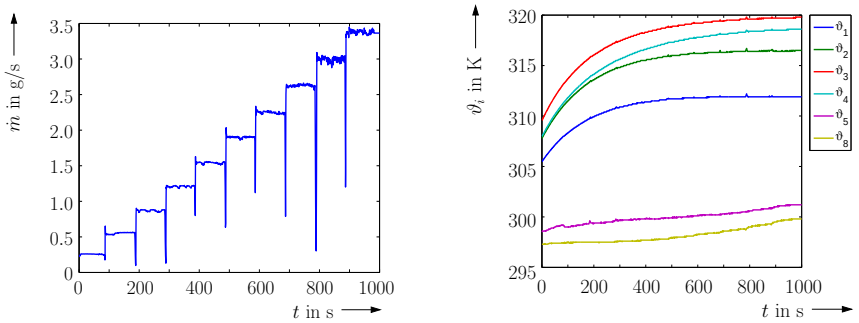

(a) Variation of the control input $\dot{m}(t)$. (b) Temperature measurements.

Fig. 7: Control inputs and measured data for the parameter identification.

online and to select the best suitable controlled variable for output feedback if the maximum internal temperature in the rod is to be controlled.

For non-quasi-linear systems, it is not guaranteed in all cases that the procedure in Subsection 6.3 leads directly to a set of hidden algebraic constraints which can be used directly to compute consistent feedforward control strategies. In this case, it is necessary to introduce dynamic extensions of the state equations. A further class of systems for which this is the case are differentially flat, multiple-input multiple-output systems for which the sum of the relative degrees[1] of the system outputs is larger than the dimension of the state vector, see Section 8. For such systems, dynamic extensions are usually necessary to derive feedforward control laws in such a way that the physical output quantities coincide with predefined trajectories.

For practical applications, the finite-volume models studied in this section are not the only possible representation that can be used for control and estimator synthesis on the basis of a finite-dimensional approximation to the PDE characterizing heat and mass transfer problems. In [12, 23, 28], further modeling approaches were derived which led to sets of ODEs for the description of temperature distributions in applications such as the considered heating systems. Thus, for all of these models, verified approaches can be used to identify the most suitable mathematical system representation for robust control synthesis and sensitivity analysis with respect to uncertain parameters.

[1] In control engineering, the relative degree of an output y_i is defined as the smallest order δ_i of its time derivative $d^{(\delta_i)}y_i/dt^{(\delta_i)}$ which explicitly depends on a considered system input.

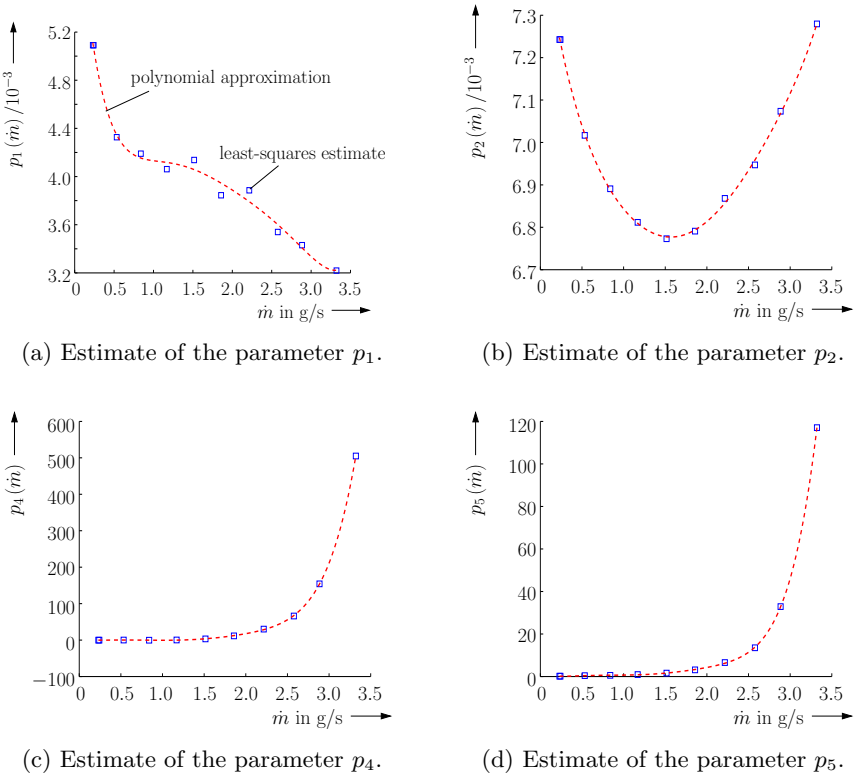

(a) Estimate of the parameter p_1.

(b) Estimate of the parameter p_2.

(c) Estimate of the parameter p_4.

(d) Estimate of the parameter p_5.

Fig. 8: Results of experimental parameter identification.

8 Dynamic Extensions for Feedforward Control Design

In this section, we demonstrate the basic procedure for dynamic extension of system models for the design of exact feedforward control strategies using the example of an autonomous robot. The investigation of possibilities to automatize this procedure in the framework of verified DAE solvers is a subject for future research.

8.1 Example — Modeling of an Autonomous Robot

Consider the autonomous robot in Fig. 10. Its equations of motion on the $(x_1\,;\,x_2)$–plane with the translational velocity u_1 and the angular velocity u_2 as inputs are given by the ODEs

$$\dot{x}\,(t) = \begin{bmatrix} \cos\left(x_3\,(t)\right) \\ \sin\left(x_3\,(t)\right) \\ 0 \end{bmatrix} u_1\,(t) + \begin{bmatrix} 0 \\ 0 \\ 1 \end{bmatrix} u_2\,(t) \quad . \tag{58}$$

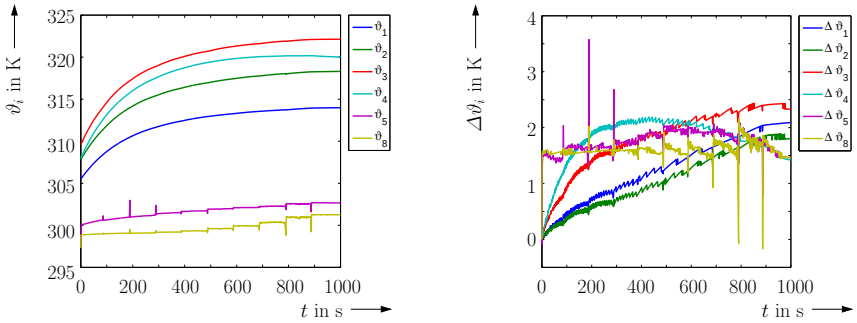

(a) Simulation of temperatures.

(b) Deviation between measured and simulated temperatures.

Fig. 9: Comparison between measured and simulated temperatures in the rod and in the air canal.

In these state equations x_3 denotes the angle of the orientation of the robot according to Fig. 10.

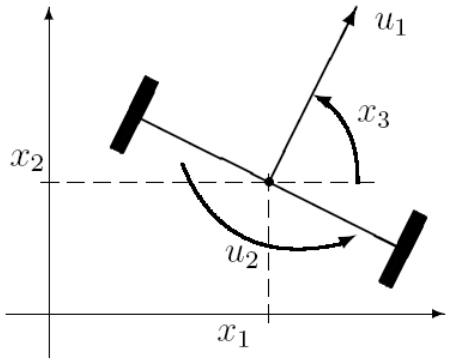

Fig. 10: Control of an autonomous robot.

In the following, we consider the computation of feedforward control strategies for the inputs u_1 and u_2 such that the actual position of the robot is consistent with a predefined trajectory $(x_{1,d}\ ;\ x_{2,d})$. Obviously, we have to assume consistent initial positions $x_1(0) = x_{1,d}(0)$ and $x_2(0) = x_{2,d}(0)$ for this task.

8.2 Feedforward Control Design

To determine dependencies of all system states $x_1(t)$, $x_2(t)$, $x_3(t)$ and all inputs $u_1(t)$, $u_2(t)$ on the desired trajectories $x_{1,d}(t)$, $x_{2,d}(t)$, both output equations $y_1 = x_1$ and $y_2 = x_2$ have to be differentiated twice. The relative degrees of the control input u_2 are equal to $\delta_1 = \delta_2 = 2$ in both cases according to

$$\begin{aligned} \dot{x}_1(t) &= \cos(x_3(t))\, u_1(t) \\ \ddot{x}_1(t) &= -\sin(x_3(t))\, \dot{x}_3(t)\, u_1(t) + \cos(x_3(t))\, \dot{u}_1(t) \\ &= -\sin(x_3(t))\, u_2(t)\, u_1(t) + \cos(x_3(t))\, \dot{u}_1(t) \end{aligned} \tag{59}$$

and

$$\begin{aligned} \dot{x}_2(t) &= \sin(x_3(t))\, u_1(t) \\ \ddot{x}_2(t) &= \cos(x_3(t))\, \dot{x}_3(t)\, u_1(t) + \sin(x_3(t))\, \dot{u}_1(t) \\ &= \cos(x_3(t))\, u_2(t)\, u_1(t) + \sin(x_3(t))\, \dot{u}_1(t) \quad . \end{aligned} \tag{60}$$

Thus, for this system there are four constraints but only three unknowns (x_3,u_1,u_2). In order to solve this problem, we extend the dynamical system model (58) with an additional state variable for the input u_1 which appears as the the first derivative $\dot{u}_1$ in the equations for both $\ddot{x}_1$ and $\ddot{x}_2$. Thus, we obtain the new system model

$$\dot{z}(t) = \begin{bmatrix} \cos(z_3(t)) \\ \sin(z_3(t)) \\ 0 \\ 0 \end{bmatrix} z_4(t) + \begin{bmatrix} 0 \\ 0 \\ 0 \\ 1 \end{bmatrix} \nu_1(t) + \begin{bmatrix} 0 \\ 0 \\ 1 \\ 0 \end{bmatrix} \nu_2(t) \tag{61}$$

with the state variables $z_1 := x_1$, $z_2 := x_2$, $z_3 := x_3$, $z_4 := u_1$. The differentiation of the output equations now leads to

$$\begin{aligned} \dot{z}_1(t) &= \cos(z_3(t))\, z_4(t) \\ \ddot{z}_1(t) &= -\sin(z_3(t))\, \dot{z}_3(t)\, z_4(t) + \cos(z_3(t))\, \dot{z}_4(t) \\ &= -\sin(z_3(t))\, z_4(t)\, \nu_2(t) + \cos(z_3(t))\, \nu_1(t) \end{aligned} \tag{62}$$

and

$$\begin{aligned} \dot{z}_2(t) &= \sin(z_3(t))\, z_4(t) \\ \ddot{z}_2(t) &= \cos(z_3(t))\, \dot{z}_3(t)\, z_4(t) + \sin(z_3(t))\, \dot{z}_4(t) \\ &= \cos(z_3(t))\, z_4(t)\, \nu_2(t) + \sin(z_3(t))\, \nu_1(t) \end{aligned} \tag{63}$$

with the new control inputs $\nu_1(t)$ and $\nu_2(t)$. These controls as well as the states $z_3(t)$ and $z_4(t)$ can be computed in the feedforward control design by substituting the desired trajectories $x_{1,d}(t)$ and $x_{2,d}(t)$ for $x_1(t)$ and $x_2(t)$, respectively.

This procedure is typical for non-quasi-linear DAE systems and, generally, for differentially flat systems for which the sum of the relative degrees exceeds the dimension of the state vector. For the extended system (61), the feedforward control and state estimation procedures introduced in Section 4 can be applied. A systematic procedure for dynamic extension of state equations in control and estimator design according to the scheme presented in this section will be developed in future work for more general application scenarios.

9 Conclusions and Outlook on Future Research

In this paper, interval-based approaches for the verification and implementation of robust control strategies were presented and applied to a finite volume representation of a distributed heating system. For this system, the online computation of feedforward control using ValEncIA-IVP was extended by a classical output feedback for compensation of model and parameter uncertainties and neglected disturbances. Furthermore, a verified estimation procedure for internal system states and disturbances was described. It is implemented using a one-stage approach instead of the classical two-stage procedure usually employed by other interval observers. This observer can be applied to verify the admissibility and reliability of classical non-verified observers such as Luenberger-type observers. For that purpose, the non-verified estimates are compared with the verified error bounds obtained in the interval approach.

In future work, we will investigate further relations between reachability and controllability of states and the solvability of DAEs describing feedforward control problems. Moreover, we will generalize the routine implemented in ValEncIA-IVP for the detection of hidden algebraic constraints. The goal will be to extend the presented automated feedforward control to multiple-input multiple-output systems for which desired output trajectories are prescribed for non-flat outputs and for which ambiguities in the solution might exist. Finally, combinations with verified tools for stability analysis based on interval evaluation of Lyapunov functions will be developed further to prove stability of non-observable or non-controllable internal dynamics and simultaneously to adapt controller structures to ensure asymptotically stable behavior.

References

1. E. Auer, A. Rauh, E.P. Hofer, and W. Luther. Validated Modeling of Mechanical Systems with SmartMOBILE: Improvement of Performance by ValEncIA-IVP. In *Proc. of Dagstuhl Seminar 06021: Reliable Implementation of Real Number Algorithms: Theory and Practice*, Lecture Notes in Computer Science, pages 1–27, 2008.
2. C. Bendsten and O. Stauning. FADBAD++, Version 2.1, 2007. `http://www.fadbad.com`.
3. M. Berz and K. Makino. COSY INFINITY Version 8.1. User's Guide and Reference Manual. Technical Report MSU HEP 20704, Michigan State University, 2002.
4. N. Delanoue. *Algoritmes numériques pour l'analyse topologique — Analyse par intervalles et théorie des graphes.* PhD thesis, École Doctorale d'Angers, 2006. In French.
5. M. Fliess, J. Lévine, P. Martin, and P. Rouchon. Flatness and Defect of Nonlinear Systems: Introductory Theory and Examples. *International Journal of Control*, 61:1327–1361, 1995.
6. M. Freihold and E.P. Hofer. Derivation of Physically Motivated Constraints For Efficient Interval Simulations Applied to the Analysis of Uncertain Dynamical Systems. *Special Issue of the International Journal of Applied Mathematics and*

Computer Science AMCS, "Verified Methods: Applications in Medicine and Engineering", 19(3):485–499, 2009.
7. A. Griewank. *Evaluating Derivatives: Principles and Techniques of Algorithmic Differentiation*. SIAM, Philidelphia, 2000.
8. L. Jaulin, M. Kieffer, O. Didrit, and É. Walter. *Applied Interval Analysis*. Springer–Verlag, London, 2001.
9. Ch. Keil. PROFIL/BIAS, Version 2.0.8, 2008. `www.ti3.tu-harburg.de/keil/profil/`.
10. H. K. Khalil. *Nonlinear Systems*. Prentice-Hall, Upper Saddle River, New Jersey, 3rd edition, 2002.
11. M. Kletting, A. Rauh, H. Aschemann, and E.P. Hofer. Interval Observer Design Based on Taylor Models for Nonlinear Uncertain Continuous-Time Systems. In *CD-Proc. of the 12th GAMM-IMACS International Symposium on Scientific Computing, Computer Arithmetic, and Validated Numerics SCAN 2006*, Duisburg, Germany, 2007. IEEE Computer Society.
12. G.V. Kostin, V.V. Saurin, A. Rauh, and H. Aschemann. Approaches to Control Design and Optimization in Heat Transfer Problems. *Izvestiya RAN. Teoriya i sistemy upravleniya (Journal of Computer and Systems Sciences International*, 2010. accepted.
13. R. Krawczyk. Newton-Algorithmen zur Bestimmung von Nullstellen mit Fehlerschranken. *Computing*, 4:189–201, 1969. In German.
14. M. Lerch, G. Tischler, J. Wolff von Gudenberg, W. Hofschuster, and W. Krämer. The Interval Library `filib++ 2.0` : Design, Features and Sample Programs. Technical Report 2001/4, Bergische Universität GH Wuppertal, 2001.
15. Y. Lin and M.A. Stadtherr. Validated solution of initial value problems for ODEs with interval parameters. In *NSF Workshop Proceeding on Reliable Engineering Computing*, Savannah GA, February 22-24 2006.
16. H.J. Marquez. *Nonlinear Control Systems*. John Wiley & Sons, Inc., New Jersey, 2003.
17. R.E. Moore. *Interval Arithmetic*. Prentice-Hall, Englewood Cliffs, New Jersey, 1966.
18. N.S. Nedialkov. Interval Tools for ODEs and DAEs. In *CD-Proc. of the 12th GAMM-IMACS International Symposium on Scientific Computing, Computer Arithmetic, and Validated Numerics SCAN 2006*, Duisburg, Germany, 2007. IEEE Computer Society.
19. N.S. Nedialkov and J.D. Pryce. Solving Differential-Algebraic Equations by Taylor Series (I): Computing Taylor Coefficients. *BIT*, 45(3):561–591, 2005.
20. N.S. Nedialkov and J.D. Pryce. Solving Differential-Algebraic Equations by Taylor Series (II): Computing the System Jacobian. *BIT*, 47(1):121–135, 2007.
21. N.S. Nedialkov and J.D. Pryce. DAETS — Differential-Algebraic Equations by Taylor Series , 2008. `http://www.cas.mcmaster.ca/~nedialk/daets/`.
22. N.S. Nedialkov and J.D. Pryce. Solving Differential-Algebraic Equations by Taylor Series (III): the DAETS Code. *J. Numerical Analysis, Industrial and Applied Mathematics*, 3:61–80, 2008.
23. A. Rauh, H. Aschemann, and V. Naumov. Experimental Validation of Flatness-Based Control for Distributed Heating Systems. In *Proc. of Days of Mechanics*, Varna, Bulgaria, 2009.
24. A. Rauh, E. Auer, and H. Aschemann. Real-Time Application of Interval Methods for Robust Control of Dynamical Systems. In *CD-Proc. of IEEE Intl. Conference on Methods and Models in Automation and Robotics MMAR 2009*, Miedzyzdroje, Poland, 2009.

25. A. Rauh, E. Auer, M. Freihold, E.P. Hofer, and H. Aschemann. Detection and Reduction of Overestimation in Guaranteed Simulations of Hamiltonian Systems. In *Proc. of the 13th GAMM-IMACS International Symposium on Scientific Computing, Computer Arithmetic, and Validated Numerics SCAN 2008 in Special Issue of Reliable Computing*, El Paso, Texas, USA, 2010.
26. A. Rauh, M. Brill, and C. Günther. A Novel Interval Arithmetic Approach for Solving Differential-Algebraic Equations with VALENCIA-IVP. *Special Issue of the International Journal of Applied Mathematics and Computer Science AMCS, "Verified Methods: Applications in Medicine and Engineering"*, 19(3):381–397, 2009.
27. A. Rauh and E.P. Hofer. Interval Methods for Optimal Control. In A. Frediani and G. Buttazzo, editors, *Proc. of the 47th Workshop on Variational Analysis and Aerospace Engineering 2007*, pages 397–418, School of Mathematics, Erice, Italy, 2009. Springer–Verlag.
28. A. Rauh, G.V. Kostin, H. Aschemann, V.V. Saurin, and V. Naumov. Verification and Experimental Validation of Flatness-Based Control for Distributed Heating Systems. *International Review of Mechanical Engineering*, 2010. accepted.
29. A. Rauh, J. Minisini, and H. Aschemann. Interval Arithmetic Techniques for the Design of Controllers for Nonlinear Dynamical Systems with Applications in Mechatronics — Part 1. *Izvestiya RAN. Teoriya i sistemy upravleniya (Journal of Computer and Systems Sciences International)*, 2010. under review.
30. A. Rauh, J. Minisini, and H. Aschemann. Interval Arithmetic Techniques for the Design of Controllers for Nonlinear Dynamical Systems with Applications in Mechatronics — Part 2. *Izvestiya RAN. Teoriya i sistemy upravleniya (Journal of Computer and Systems Sciences International)*, 2010. under review.
31. A. Rauh, J. Minisini, and E.P. Hofer. Towards the Development of an Interval Arithmetic Environment for Validated Computer-Aided Design and Verification of Systems in Control Engineering. In *Proc. of Dagstuhl Seminar 08021: Numerical Validation in Current Hardware Architectures*, volume 5492 of *Lecture Notes in Computer Science*, pages 175–188, Dagstuhl, Germany, 2008. Springer–Verlag.
32. A. Rauh, J. Minisini, and E.P. Hofer. Verification Techniques for Sensitivity Analysis and Design of Controllers for Nonlinear Dynamic Systems with Uncertainties. *Special Issue of the International Journal of Applied Mathematics and Computer Science AMCS, "Verified Methods: Applications in Medicine and Engineering"*, 19(3):425–439, 2009.
33. A. Rauh, J. Minisini, E.P. Hofer, and H. Aschemann. Robust and Optimal Control of Uncertain Dynamical Systems with State-Dependent Switchings Using Interval Arithmetic. In *Proc. of the 13th GAMM-IMACS International Symposium on Scientific Computing, Computer Arithmetic, and Validated Numerics SCAN 2008 in Special Issue of Reliable Computing*, El Paso, Texas, USA, 2010.
34. J. Rohn. Positive Definiteness and Stability of Interval Matrices. *SIAM Journal on Matrix Analysis and Applications*, 15(1):175–184, 1994.